scientific reports

Check for updates

OPEN

Targeted pancreatic cancer therapy using 4-farnesyloxycoumarin conjugated nanocrystalline cellulose and Chitosan nanoparticles

Fariba Karoonkiani[1], Masoud Homayouni Tabrizi[2]✉, Mohammad Taghi Goodarzi[3] & Alireza Jalali[1]

This study investigates the effects of 4-farnesyloxycoumarin (4-FOC)-conjugated NCC/CTAB/CS nanoparticles (NPs) on PANC-1 pancreatic cancer cells, highlighting their cytotoxicity and antioxidant properties. Dynamic light scattering (DLS) analysis revealed a Z-average particle size of 275.68 nm, with a polydispersity index of 0.3020. The mean intensity diameter was 334.68 nm, and the mean volume diameter was 380.97 nm. The zeta potential was recorded at 28.88 ± 12.64 mV, confirming good stability due to electrostatic repulsion. Field emission scanning electron microscopy (FESEM) confirmed the successful conjugation of 4-FOC to the NPs, and Fourier-transform infrared (FTIR) spectroscopy validated the incorporation of functional groups. In contrast, the encapsulation efficiency of 4-FOC was measured at 88.49%. Cytotoxicity assays indicated a significant reduction in PANC-1 cell viability, with an IC50 value of 61.23 µg/mL; in contrast, human dermal fibroblast (HDF) cells exhibited greater resilience, maintaining 92.61 ± 2.33% viability at 100 µg/mL. Apoptotic assays revealed a dose-dependent increase in early and late apoptotic cells, with late apoptosis rising to 54.1% at 81 µg/mL. Gene expression analysis showed significant upregulation of caspase 3 (2.25 ± 0.33), p21 (1.70 ± 0.05), and p53 (2.71 ± 0.29 at 61 µg/mL), underscoring the NPs' role in apoptosis and cell cycle regulation. Additionally, the antioxidant capacity of the NPs was confirmed through ABTS and DPPH radical scavenging assays, achieving 38.82% and 68.25% scavenging activity at the highest concentrations, respectively. These findings suggest that 4-FOC-conjugated NCC/CTAB/CS NPs hold promise as a therapeutic strategy for treating pancreatic cancer.

Keywords 4-Farnesyl oxy coumarin, Nanoparticles, Pancreatic neoplasms, Antioxidants, Cytotoxicity, Apoptosis

Targeted therapy is a significant advancement in cancer treatment, focusing on specific molecular targets and signaling pathways associated with various cancers[1]. Unlike traditional chemotherapy, which affects both cancerous and healthy cells, targeted therapy aims to minimize damage to normal tissues and reduce side effects[2]. A critical component of effective targeted therapies is the development of drug delivery systems (DDSs), which include nanoparticles (NPs), liposomes, and micelles designed to deliver therapeutic agents directly to tumor sites[3–5]. These systems enhance drug bioavailability and stability, ensuring higher concentrations reach the tumor while minimizing systemic exposure and reducing the risk of drug resistance[6]. The continued development of sophisticated drug carriers promises more effective and personalized cancer treatments.

Among the various DDS, nanocrystalline cellulose/cetyltrimethylammonium bromide/chitosan (NCC/CTAB/CS) NPs present a promising platform for cancer therapy[7–9]. These NPs possess unique structural properties and biocompatibility, which improve their interaction with the tumor microenvironment. Nanocrystalline cellulose (NCC), a renewable biopolymer, exhibits high surface area and biodegradability, making it an excellent nanocarrier for hydrophobic drugs[10,11]. Incorporating cetyltrimethylammonium bromide

[1]Department of Chemistry, Shahrood Branch, Islamic Azad University, Shahrood, Iran. [2]Department of Biology, Mashhad Branch, Islamic Azad University, Mashhad, Iran. [3]Department of Biochemistry, Shahrood Branch, Islamic Azad University, Shahrood, Iran. ✉email: mhomayouni6@gmail.com

(CTAB), a cationic surfactant, improves the solubility and stabilization of the nanoparticles, facilitating sustained drug release and enhancing cellular uptake[8,12]. Additionally, chitosan (CS), a biocompatible and biodegradable natural polysaccharide, can encapsulate chemotherapeutic agents, improving their stability and bioavailability[13]. Additionally, CS disrupts tight junctions in epithelial tissues, enhancing drug absorption[14]. Therefore, incorporating CS into NCC/CTAB NPs may facilitate targeted therapy. This targeted approach increases the treatment efficacy and minimizes side effects, making CS a promising candidate for effective cancer therapies.

The present study aimed to evaluate the effects of 4-farnesyloxycoumarin (4-FOC) conjugated with NCC/CTAB/CS NPs on the human pancreatic cancer cell line PANC-1. FOC, a coumarin derivative, shows promising potential in cancer treatment due to its ability to induce apoptosis and inhibit the proliferation of cancer cells[15–17]. Coumarins, secondary metabolites found in plants of the Apiaceae and Rutaceae families, are characterized by a benzene ring, an alpha-pyrone, and a carbonyl group[18]. Coumarins' conjugated double bonds enable them to scavenge free radicals and engage in non-covalent interactions like hydrogen bonding and van der Waals forces[19]. FOC derivatives primarily inhibit the enzyme 15-lipoxygenase-1 (15-LOX-1), often overexpressed in prostate cancer[20]. They also show promising anti-cancer effects by inducing apoptosis and inhibiting proliferation through modulation of signaling pathways like MAPK and NF-κB[21]. However, their low bioavailability and low efficiency in targeting cancer cells challenge the clinical application of FOC derivatives. The lipophilic nature of FOC derivatives can hinder their absorption and distribution within the body[22,23]. Thus, creating new DDSs is crucial for improving the treatment efficacy of FOC derivatives and reducing side effects.

The present study aims to elucidate the impact of 4-FOC-conjugated NCC/CTAB/CS NPs on PANC-1 cells, a model for pancreatic ductal adenocarcinoma known for its aggressive nature and resistance to apoptosis. This study presents a novel approach to enhancing the therapeutic efficacy of 4-FOC in pancreatic cancer treatment by utilizing a unique DDS composed of NCC/CTAB/CS nanoparticles. By conjugating 4-FOC with these nanoparticles, we aim to overcome the challenges of low bioavailability and ineffective targeting associated with traditional formulations. Incorporating NCC, CTAB, and chitosan improves the solubility and stability of the therapeutic agent and enhances cellular uptake and targeted delivery to PANC-1 cells, a model for aggressive pancreatic ductal adenocarcinoma. This innovative DDS strategy seeks to maximize the anti-cancer properties of 4-FOC while minimizing side effects, paving the way for more effective and personalized cancer therapies.

Materials and methods

Chemicals

In this study, various chemicals were utilized, including microcrystalline cellulose (MCC) powder from Sigma-Aldrich, 64% sulfuric acid and CTAB from Merck, and acetic acid (≥ 99.7%) also from Merck. Dimethyl sulfoxide (DMSO) and MTT reagent (5 mg/mL) were sourced from Merck, while the Annexin V-FITC/PI apoptosis staining detection kit was obtained from Abcam (ab14085). Acridine orange (AO), propidium iodide (PI), and DAPI were all acquired from Sigma-Aldrich. RNA extraction was performed using a QIAGEN kit, with Moloney Murine Leukemia Virus Reverse Transcriptase from Promega and Bio-Rad SYBR Green Master Mix for real-time PCR. Additionally, potassium persulfate and glutathione were sourced from Merck, ensuring high-quality reagents for the experiments.

Fabrication of 4-FOC-conjugated NCC/CTAB/CS NPs

NCC was synthesized by treating 10 g of MCC powder with 64% sulfuric acid. The mixture was incubated at 60 °C for 90 min. The process was then halted by adding 800 mL of cold distilled water, followed by centrifugation and washing to eliminate excess acid. The resulting suspension underwent dialysis for 7 days to remove low-molecular-weight byproducts, followed by ultrasonic dispersion to achieve homogeneity. The final product, a white suspension, was then lyophilized to obtain the dry NCC.

To functionalize the NCC with CTAB, 200 mg of NCC was mixed with 4 μM CTAB in an aqueous solution and stirred at 60 °C for 3 h. Unreacted CTAB was then removed by centrifugation. The 4-FOC solution was introduced into the NCC-CTAB mixture under continuous stirring to achieve uniform distribution. The dispersion was then centrifuged and lyophilized. Finally, CS was dissolved in a 1% acetic acid solution (≥ 99.7%) and incorporated into the 4-FOC-conjugated NCC/CTAB dispersion. This mixture was incubated for 24 h, followed by centrifugation and lyophilization to obtain the final product[7,8,24].

Characterization of 4-FOC-conjugated NCC/CTAB/CS NPs

Dynamic light scattering (DLS) (Microtrac) was used to characterize the hydrodynamic size and distribution of the particles in aqueous solution[25]. This method allows for assessing the particle size distribution and stability in suspension. Field emission scanning electron microscopy (FESEM) (Hitachi) was used to examine particle morphology, and Fourier transform infrared spectroscopy (FTIR) analysis (Perkin-Elmer) was performed to investigate functional groups.

Cytotoxicity assay

The cytotoxic effects of 4-FOC-conjugated NCC/CTAB/CS NPs on PANC-1 cancer cells (Institut Pasteur, Iran) and human dermal fibroblast (HDF) cells (Institut Pasteur, Iran) were evaluated using the MTT assay. Cells were seeded at a density of 1×10^4 in 96-well plates for 24 h. Following incubation, cells were treated with NCC/CTAB/CS NPs at concentrations of 1.6, 3.1, 6.2, 12.5, 25, 50, and 100 μg/mL. After a 48-hour incubation, 20 μL of MTT reagent (5 mg/mL) was added to each well and incubated for 4 hours in the dark at 37 °C. After removing the medium, 200 μL of DMSO was added to dissolve the formazan crystals, followed by a 1-hour incubation. Finally, absorbance was measured at 570 nm using a microplate reader. The percentage of cell viability was calculated for the control group.

Annexin V-FITC/PI assay

The Annexin V-FITC apoptosis staining detection kit was used to assess apoptosis per the manufacturer's instructions. After exposing PANC-1 cells to 4-FOC-conjugated NCC/CTAB/CS NPs at concentrations of 31, 61, and 81 µg/mL for 48 h, the cells were trypsinized and centrifuged. A sample of 1 × 10^5 cells was resuspended in 500 µl of binding buffer and incubated with 5 µl of annexin V-FITC and 5 µl of PI at 25 °C for 5 min in the dark. The cells were then resuspended in 400 µl of binding buffer and analyzed by flow cytometry to assess early apoptotic (Annexin V+, PI-), late apoptotic (Annexin V+, PI+), and necrotic (Annexin V-, PI+) cells. The 61 µg/mL concentration represents the IC50, while 31 and 61 µg/mL concentrations were selected to induce cell death at approximately 25% and 75%, respectively.

AO/PI staining

PANC-1 cells were seeded at a density of 1×10^4 cells per well in 6-well plates and incubated for 24 h. After incubation, the cells were treated with 4-FOC-conjugated NCC/CTAB/CS NPs at 31, 61, and 81 µg/mL concentrations for 48 h. After the treatment, the cells were trypsinized and washed with phosphate-buffered saline (PBS). They were then resuspended in a PBS solution containing AO at a concentration of 1 µg/mL and PI at a concentration of 5 µg/mL and incubated at room temperature for 10 min. Finally, the cells were rewashed and examined under a fluorescence microscope (Carl Zeiss, Jena, Germany).

DAPI staining

To assess apoptosis in PANC-1 cells treated with 4-FOC-conjugated NCC/CTAB/CS NPs at 31, 61, and 81 concentrations for 48 h, we employed the DAPI staining. After treatment, cells were washed with PBS, fixed in 4% paraformaldehyde for 15 min, and permeabilized with 0.1% Triton X-100 for 10 min. Following another PBS wash, cells were incubated with 1 µg/mL DAPI for 5 min in the dark, rewashed, and examined under a fluorescence microscope.

Real-time polymerase chain reaction (real time-PCR)

The mRNA expression levels of caspase 3, superoxide dismutase (SOD), P21, and P53 were assessed using real-time PCR. RNA was extracted from PANC-1 cells using a QIAGEN kit and quantified using a ThermoFisher Nanodrop ND-1000. The extracted mRNA was converted to complementary DNA (cDNA) using Moloney Murine Leukemia Virus Reverse Transcriptase (Promega). Real-time PCR was performed with a Corbett thermal cycler, specific primers (Table 1), and Bio-Rad SYBR Green Master Mix. The comparative Ct (cycle threshold) method was employed to normalize the gene expression levels, using glyceraldehyde-3-phosphate dehydrogenase (GAPDH) as the reference gene. Mean Ct values from triplicate samples were analyzed using the $2^{-\Delta\Delta Ct}$ formula.

Antioxidant activity assay

The antioxidant capacity of 4-FOC-conjugated NCC/CTAB/CS NPs was assessed using the ABTS and DPPH assays, with glutathione as a control. For the ABTS assay, a stock solution of 7 mM ABTS and 2.45 mM potassium persulfate was incubated in the dark for 12 h and diluted to an absorbance of 0.70 at 734 nm. Various concentrations of 4-FOC-conjugated NPs were added, and absorbance was measured after 6 min. In the DPPH assay, a 0.1 mM DPPH solution in methanol was incubated for 30 min in the dark. Different concentrations of 4-FOC-conjugated NCC/CTAB/CS NPs were added, and absorbance was measured at 517 nm. Radical scavenging activity was calculated using % inhibition = (control absorbance – sample absorbance) / control absorbance × 100.

Molecular docking analysis

Molecular docking was performed using Windows 11 personal computers equipped with Intel Core i7 1165G7 processors and NVidia GeForce MX450 graphics cards, utilizing Molecular Operating Environment (MOE) 2019 software. The three-dimensional structure of the 4-FOC ($C_{24}H_{30}O$) was obtained from the PubChem database and energy-optimized with a gradient of 0.01 kcal/mol/Å. Relevant target proteins, including SNAI1 (PDB ID: 3w5k), FAK1 (PDB ID: 3BZ3), and GTPase KRas (PDB ID: 4EPV), were retrieved from the PDB repository. Protein preparation involved removing water and ligands, protonation, and minimization using the AMBER10: EHT force field. Active binding sites were identified through MOE's Site Finder tool. The docking

Primer	Sequence
Caspase 3	F: 5′-CTGGACTGTGGCATTGAGAC-3′ R: 5′-ACAAAGCGACTGGATGAACC-3′
SOD	F 5′- CAGCATGGGTTCCACGTCCA – 3′ R 5′- CACATTGGCCACACCGTCCT – 3′
P21	F 5′- AAGACCATGTGGACCTGTCACTGT-3′ R 5′- GAAGATCAGCCGGCGTTTG-3′
P53	F 5′- TCA GAT CCT AGC GTC GAG CCC-3′ R 5′- GGG TGT GGA ATC AAC CCA CAG-3′
GAPDH	F 5′- GCAGGGGGGAGCCAAAAGGGT-3′ R 5′- TGGGTGCCAGTGATGGCATGG-3′

Table 1. Specific primer sequences for real-time PCR.

process utilized the 'Induced Fit' protocol, importing the ligand in mdb format, and employed the 'Triangle Matcher/London dG' and 'Forcefield/GBVI-WSA dG' parameters for refinement. Interaction analysis and scoring were conducted post-docking, with lower S-scores indicating stronger ligand-protein binding.

Statistical analysis

Statistical analyses were performed using SPSS software (version 22). The normality of the data was assessed with the Shapiro-Wilk test. A one-way analysis of variance (ANOVA) was performed to compare multiple groups, followed by Tukey's test for subsequent comparisons to identify specific differences among the groups. A p-value of less than 0.05 was considered statistically significant. All data are presented as means ± standard deviations (SD).

Results

This study aimed to assess the effects of 4-FOC-conjugated NCC/CTAB/CS NPs on PANC-1 cells, explicitly evaluating their cytotoxicity and antioxidant capacity.

DLS assay

The DLS analysis of 4-FOC-conjugated NCC/CTAB/CS NPs revealed key characteristics indicative of their stability and size distribution (Fig. 1A). The Z-average particle size was found to be 275.68 nm, indicating a moderate size that is suitable for various biomedical applications. The polydispersity index (PDI) of 0.3020 suggests a relatively narrow size distribution, which is favorable for consistent performance in DDS. The mean intensity diameter measured 334.68 nm, and the mean volume diameter was 380.97 nm, suggesting the presence of larger aggregates. The mean number diameter of 113.57 nm indicates that a significant proportion of smaller particles could enhance the efficacy of the NPs for targeted delivery. The zeta potential recorded at 28.88 ± 12.64 mV indicates good stability due to electrostatic repulsion among the particles (Fig. 1B). Additionally, the mean electrophoretic mobility of 2.28 ± 1 confirms their potential for effective dispersion in solution. Overall, these findings emphasize the promising characteristics of the synthesized NPs for potential applications in drug delivery and nanomedicine.

FESEM

The FESEM micrograph shows a textured surface with numerous spherical NPs, indicating successful conjugation (Fig. 1C). The image shows a heterogeneous size distribution among the particles, with variations in length and diameter, indicating differences in their aggregation or formation processes. The background displays a dense, uneven texture that indicates an interconnected network of nanofibers, which is typical of nanocellulose-based materials. With a scale bar of 500 nm, the micrograph emphasizes the nanoscale nature of the materials, providing valuable insights into their physical characteristics that are essential for applications such as drug delivery and catalysis.

FTIR spectroscopy

FTIR analysis of free 4-FOC reveals its functional groups and structural features (Fig. 2A). The broad absorption band at 3395.23 cm^{-1} indicates hydroxyl groups. At the same time, peaks at 3076.50 cm^{-1} and 1625.16/1565.27 cm^{-1} correspond to C–H and C=C stretching vibrations of the aromatic rings. Peaks at 2966.17, 2912.75, and 2847.67 cm^{-1} show farnesyl moiety's aliphatic methyl and methylene groups. The peak represents the carbonyl group of the coumarin ring at 1730.04 cm^{-1}, and ether linkages are confirmed by C–O–C stretching vibrations at 1272.94 and 1248.06 cm^{-1}. C–O stretching vibrations at 1189.25, 1138.86, and 1105.58 cm^{-1} further

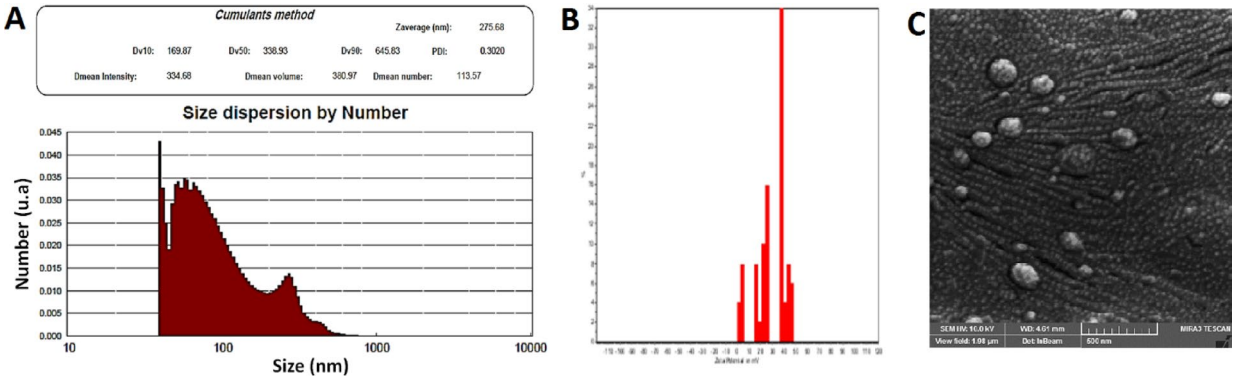

Fig. 1. DLS analysis of 4-FOC-conjugated NCC/CTAB/CS NPs. (**A**) Size distribution and stability characteristics indicate a Z-average particle size of 275.68 nm and a PDI of 0.3020, suggesting a narrow size distribution. (**B**) Zeta potential measurements show a value of 28.88 ± 12.64 mV, reflecting good stability due to electrostatic repulsion. (**C**) FESEM micrograph of 4-FOC-conjugated NCC/CTAB/CS NPs shows a textured surface with spherical NPs, indicating successful conjugation. A 500 nm scale bar highlights the nanoscale relevance for drug delivery applications. These results underscore the NPs' potential for biomedical applications.

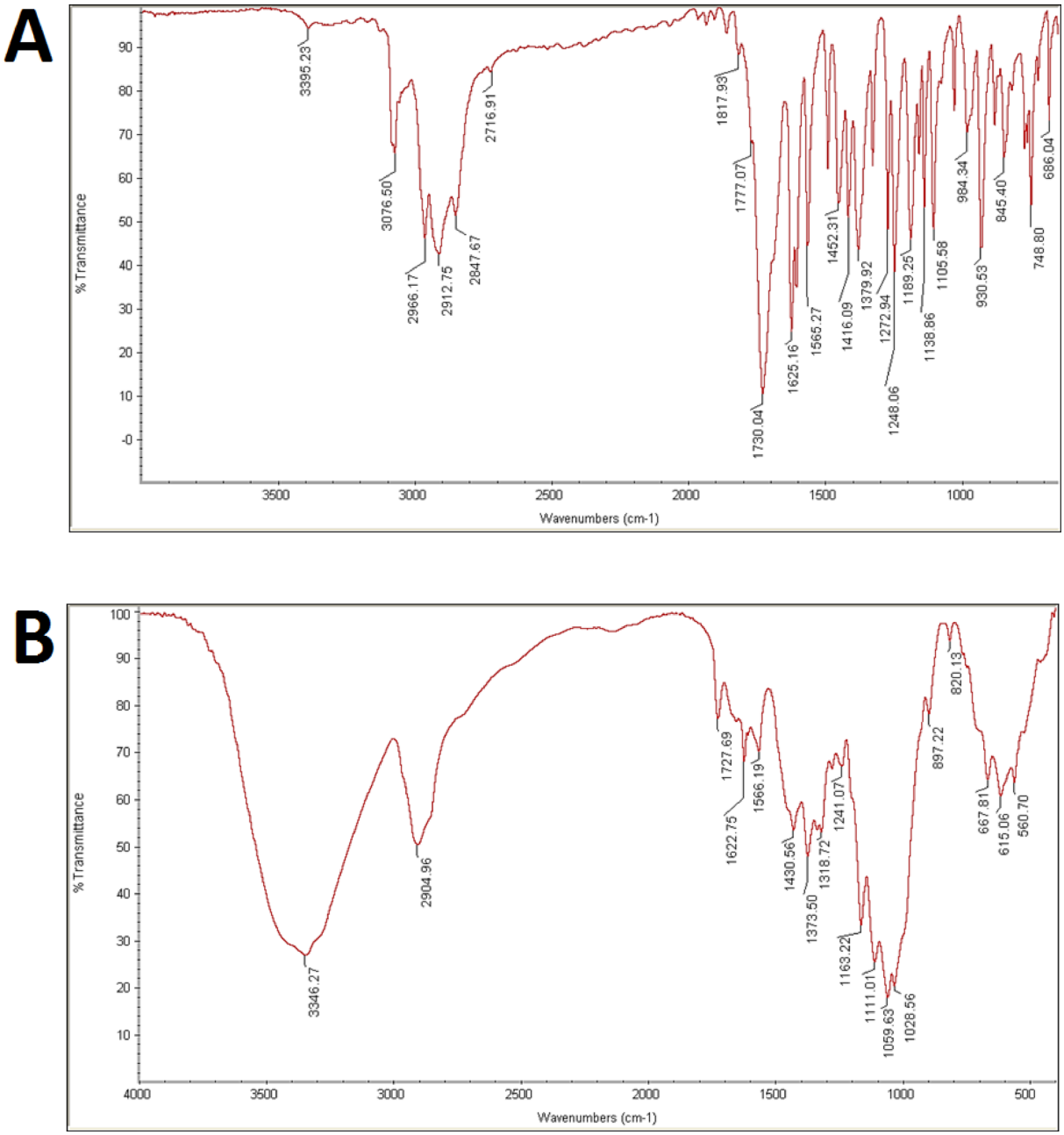

Fig. 2. FTIR spectroscopy analysis of free 4-FOC (**A**) and 4-FOC-conjugated NCC/CTAB/CS NPs (**B**). The spectra reveal that key functional groups include hydroxyl, aliphatic, and aromatic groups, along with characteristic carbonyl, ether, and ester linkages. These findings confirm the successful synthesis and integration of 4-FOC with the NPs.

support ether and ester functionalities. Out-of-plane C-H bending vibrations of the aromatic rings appear at 984.34, 930.53, 845.40, 748.80, and 686.04 cm^{-1}.

The FTIR analysis of 4-FOC-conjugated NCC/CTAB/CS NPs (Fig. 2B) shows a broad band at 3346.27 cm^{-1}, indicating hydroxyl groups from NCC and CS. The C–H stretching vibrations of aliphatic methylene groups appear at 2904.96 cm^{-1}, while the coumarin ring's carbonyl group is at 1727.69 cm^{-1}. C=C stretching vibrations from aromatic rings are at 1622.75 and 1566.19 cm^{-1}. Ether and ester linkages are confirmed by C–O–C and C–O stretching vibrations at 1318.72, 1241.07, 1163.22, and 1111.01 cm^{-1}. Peaks at 1059.63, 1028.56, and 897.22 cm^{-1} characterize NCC and CS, and out-of-plane C–H bending vibrations at 820.13 and 667.81 cm^{-1} further support the successful conjugation of 4-FOC with the NPs. This FTIR analysis confirms the successful synthesis of the NPs and the integration of functional groups.

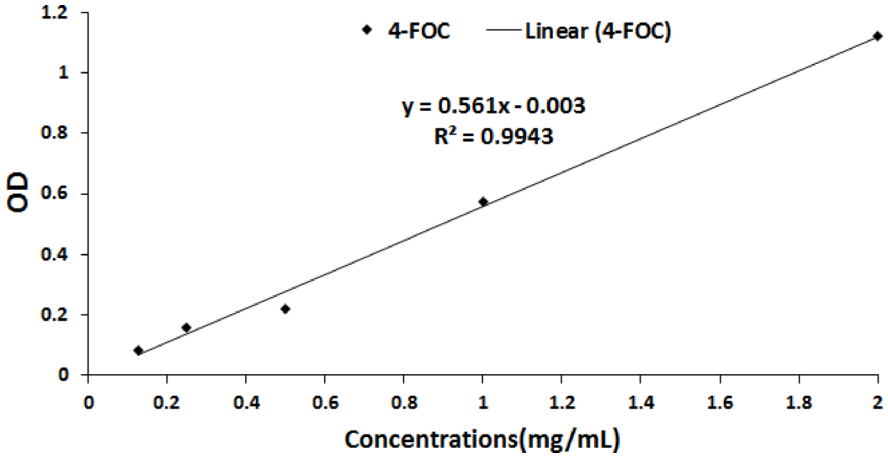

Fig. 3. The spectrophotometric assessment of encapsulation efficiency revealed an 88.49% incorporation of 4-FOC into NCC/CTAB/CS NPs.

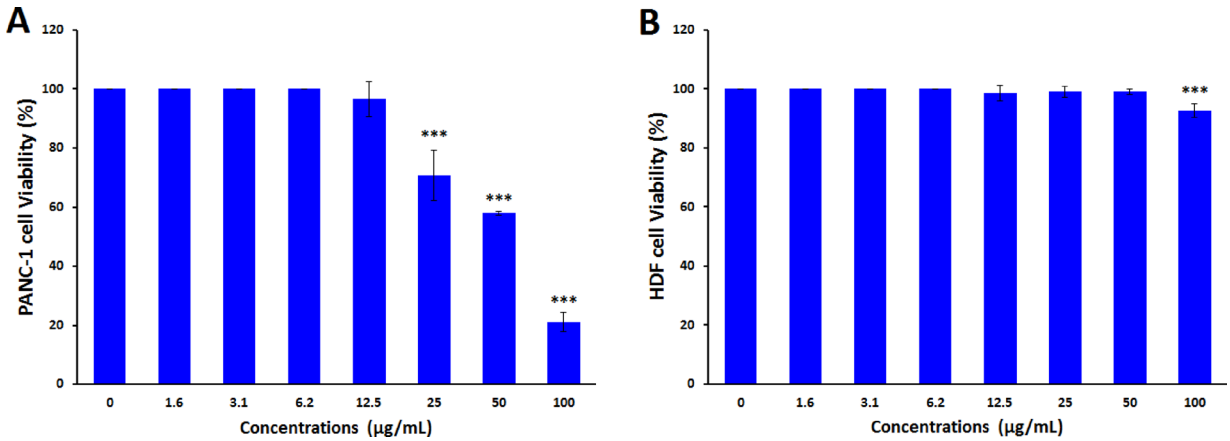

Fig. 4. Cell viability results from MTT assays on PANC-1 cells (**A**) and HDF cells (**B**) treated with varying concentrations of 4-FOC-conjugated NCC/CTAB/CS NPs. PANC-1 cells show significant reductions in viability at concentrations of 25 µg/mL and above, with an IC50 value of 61.23 µg/mL, indicating effective cytotoxicity. In contrast, HDF cells exhibit greater resilience, with minimal viability decline observed, highlighting the selective cytotoxic effect of the NPs on cancer cells. The data is presented as mean ± standard deviation (SD), and statistical significance is denoted as ** $P < 0.01$ and *** $P < 0.001$.

Encapsulation efficacy

The encapsulation efficiency was evaluated using a spectrophotometric method at a wavelength of 399 nm (Fig. 3). An efficiency of 88.49% indicates the successful incorporation of a significant amount of 4-FOC into the NCC/CTAB/CS NPs.

Cytotoxicity assay

MTT assay results showed a significant reduction in cell viability in PANC-1 cells treated with the NPs at higher concentrations (Fig. 4A). At concentrations of 0 to 6.2 µg/mL, cell viability remained at 100%. In comparison, 12.5 µg/mL treatment yielded 96.63 ± 5.83% viability. Notably, at concentrations of 25 µg/mL (70.65 ± 8.48%), 50 µg/mL (57.84 ± 0.7%), and 100 µg/mL (20.99 ± 3.27%), there was a statistically significant decrease in viability compared to the control group ($P < 0.001$). The calculated IC50 value was 61.23 µg/mL, indicating significant cytotoxicity of the NPs on PANC-1 cells.

In contrast, HDF cells exhibited a more resilient response to treatment with the same NPs (Fig. 4B). Cell viability remained at 100% for all concentrations up to 6.2 µg/mL, with a slight decrease observed at 12.5 µg/mL (98.47 ± 2.65%) and 25 µg/mL (98.98 ± 1.77%). A significant decline in viability was observed only at the highest tested concentration of 100 µg/mL (92.61 ± 2.33%) ($P < 0.001$). These findings suggest that while PANC-1 cells are significantly affected by the treatment, HDF cells show a higher tolerance to the effects of 4-FOC-conjugated NCC/CTAB/CS NPs.

Annexin V-FITC/PI assay

Figure 5 illustrates a significant dose-dependent increase in apoptotic activity following treatment with the NPs at 31, 61, and 81 µg/mL concentrations. In the untreated control cells, the percentages of early and late apoptotic cells were minimal, recorded at 0.58% and 1.62%, respectively. At a concentration of 31 µg/mL, there was a notable increase in early and late apoptotic cells, with percentages rising to 3.34% and 23.9%, respectively. At a 61 µg/mL concentration, early apoptotic cells accounted for 6.15%, while late apoptotic cells surged to 44.1%. At the highest concentration of 81 µg/mL, the figures for apoptotic populations intensified further, revealing 5.48% in early apoptosis and 54.1% in late apoptosis. These findings suggest that 4-FOC-conjugated NCC/CTAB/CS NPs effectively induce apoptosis in PANC-1 cells in a concentration-dependent manner.

AO/PI and DAPI staining

AO/PI staining of PANC-1 cells treated with varying concentrations of the NPs (31, 61, and 81 µg/mL) demonstrates distinct fluorescence patterns that correlate with treatment dosage (Fig. 6A). The untreated control cells show uniform green fluorescence, indicating a healthy, viable cell population. At the 31 µg/mL concentration, a mixed fluorescence profile emerged, with some cells displaying both green and orange/red fluorescence. It indicates the presence of viable as well as early apoptotic cells. At a concentration of 61 µg/mL, there is a notable increase in orange/red fluorescence, indicating a higher proportion of late apoptotic or necrotic cells. At the highest 81 µg/mL concentration, approximately 50% of the cells exhibit orange/red fluorescence, indicating significant induction of apoptosis and extensive cell death.

Additionally, DAPI staining confirmed that higher doses of NPs reduced cell viability (Fig. 6B). In this method, apoptotic cells displayed characteristic signs, such as nuclear condensation and fragmentation. These data indicate that 4-FOC-conjugated NCC/CTAB/CS NPs effectively induce apoptosis in PANC-1 cells, highlighting their potential as a therapy for pancreatic cancer treatment.

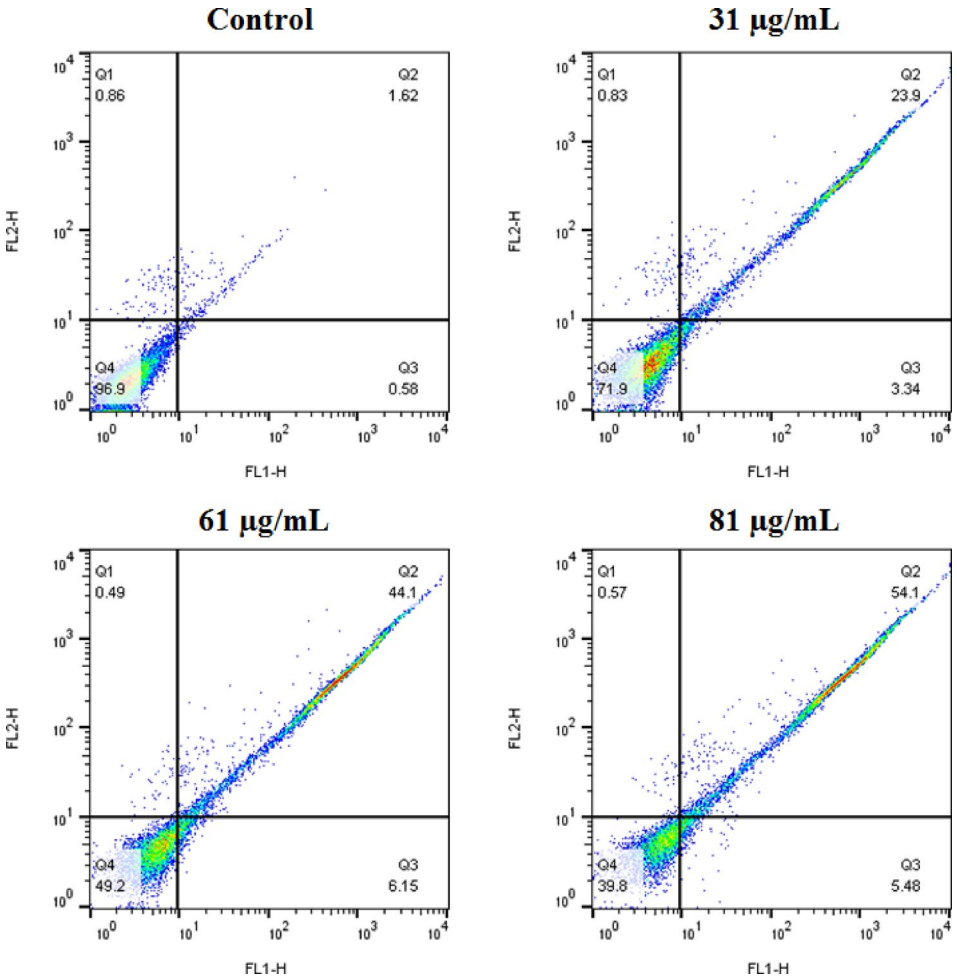

Fig. 5. Flow cytometry analysis of apoptosis in PANC-1 cells. Results showed a dose-dependent increase in apoptotic activity in PANC-1 cells following treatment with 4-FOC-conjugated NCC/CTAB/CS NPs. Apoptotic cell percentages for untreated controls were minimal (0.58% early, 1.62% late), while treatment at 31, 61, and 81 µg/mL significantly elevated early (3.34%, 6.15%, 5.48%) and late (23.9%, 44.1%, 54.1%) apoptosis rates, demonstrating effective induction of apoptosis.

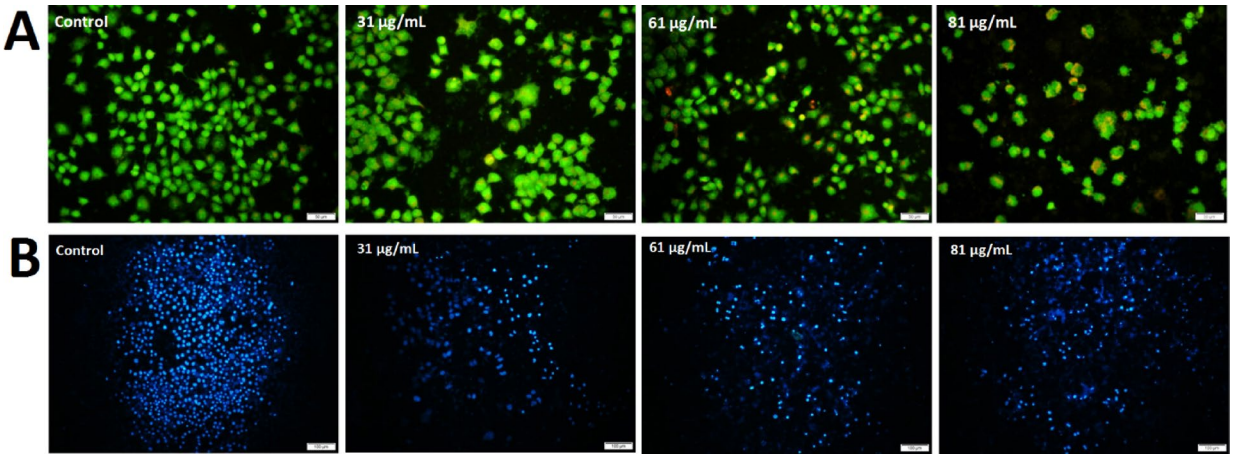

Fig. 6. AO/PI staining analysis of PANC-1 cells treated with 4-FOC-conjugated NCC/CTAB/CS NPs reveals distinct fluorescence patterns by dosage. Controls show uniform green fluorescence, while 31 µg/mL treatment indicates early apoptosis with mixed green and orange/red fluorescence. At 61 µg/mL, increased orange/red fluorescence suggests late apoptosis or necrosis, and at 81 µg/mL, about 50% of cells display orange/red fluorescence, indicating significant cell death. DAPI staining further confirms reduced viability and apoptotic features, highlighting the therapeutic potential of these NPs in pancreatic cancer.

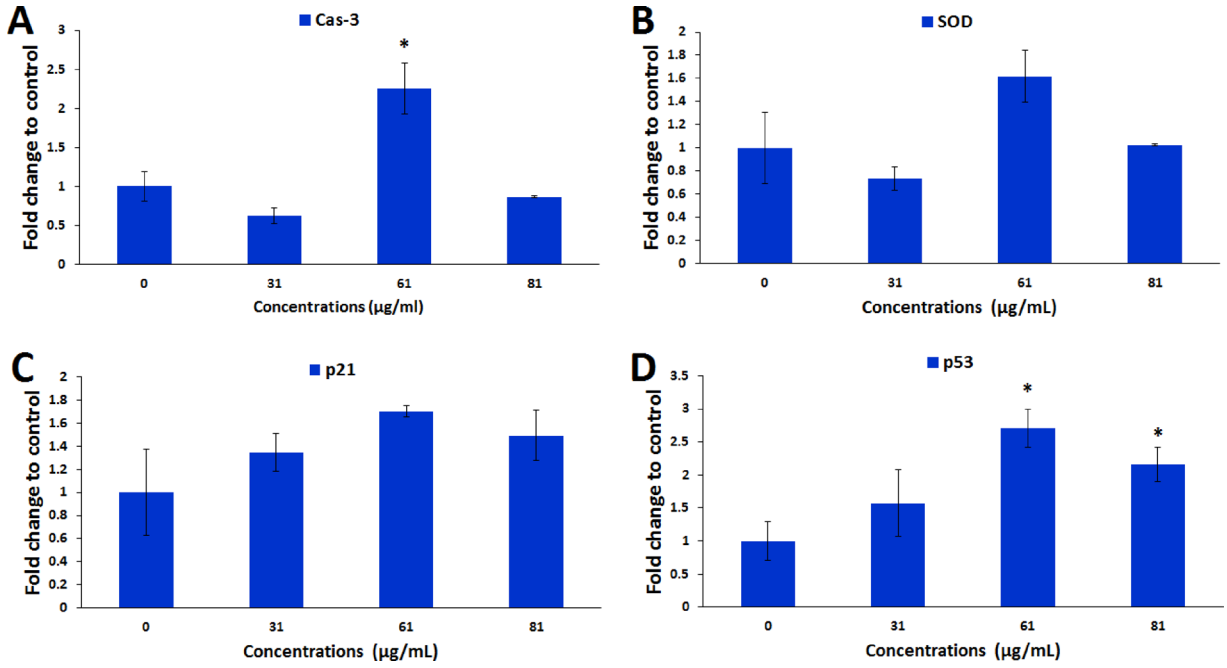

Fig. 7. Real-time PCR assay for mRNA expression of caspase 3, SOD, p21, and p53 in PANC-1 cells treated with 4-FOC-conjugated NCC/CTAB/CS NPs. At 61 µg/mL, caspase 3 expression (**A**) increased to 2.25 ± 0.33, indicating apoptosis involvement, while SOD (**B**) and p21 (**C**) upregulated, reflecting responses to oxidative stress and cell cycle regulation. p53 levels (**D**) elevated significantly at both 61 µg/mL (2.71 ± 0.29) and 81 µg/mL (2.15 ± 0.26), underscoring its role in the cellular stress response. These results suggest that 4-FOC-conjugated NCC/CTAB/CS NPs can modulate key gene expressions related to apoptosis and cell cycle regulation in a concentration-dependent manner. The data is presented as mean ± standard deviation (SD), and statistical significance is denoted as $^*P < 0.05$.

Gene expression assay

The mRNA expression levels of caspase 3, SOD, p21, and p53 in PANC-1 cells treated with different concentrations of 4-FOC-conjugated NCC/CTAB/CS NPs were evaluated using real-time PCR. At a 61 µg/mL concentration, caspase 3 expression increased significantly to 2.25 ± 0.33 ($P < 0.05$), suggesting its potential role in promoting apoptosis (Fig. 7A). Similarly, SOD expression increased at this concentration to 1.62 ± 0.22. Although this

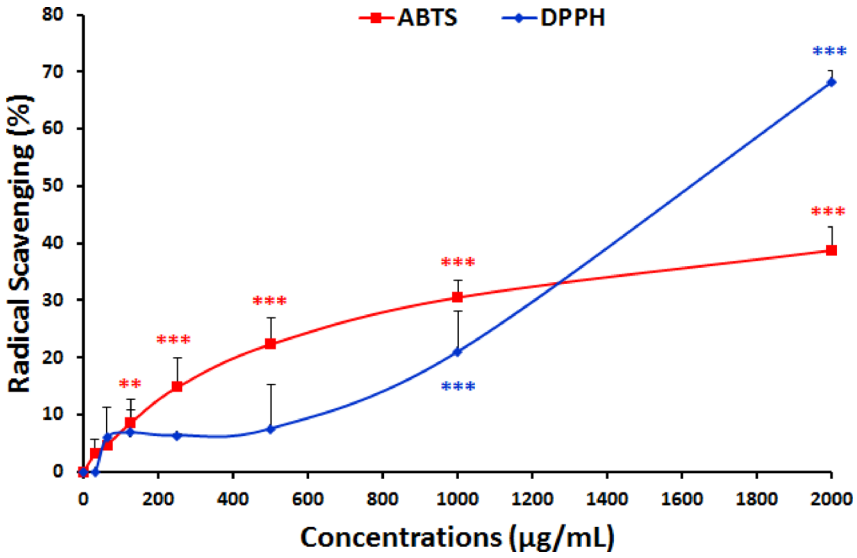

Fig. 8. Antioxidant capacity of 4-FOC-conjugated NCC/CTAB/CS NPs assessed by ABTS and DPPH radical scavenging assays. Results show a significant concentration-dependent increase in scavenging activity, with ABTS activity reaching 38.82% and DPPH activity achieving 68.25% at the highest concentration of 2000 µg/mL. These findings confirm the notable antioxidant properties of the NPs in scavenging free radicals. The data is presented as mean ± standard deviation (SD), and statistical significance is denoted as $^{**}P < 0.01$ and $^{***}P < 0.001$.

PDB ID	Complex protein-ligand	S-score	E-conformation	E-refine	Amino Acids Bonds
3w5k	Snail1-4-farnesyloxycoumarin	− 6.85	− 31.46	− 27.54	Glu565
3BZ3	Focal Adhesion Kinase-4-farnesyloxycoumarin	− 6.96	− 38.01	− 36.69	Arg426
4EPV	GTPase KRas-4-farnesyloxycoumarin	− 7.91	− 44.94	− 47.56	Ser17, Gly15, Lys16

Table 2. The S-score, binding energy, and the specific amino acids involved in the interaction between 4-farnesyloxycoumarin and the proteins Snail1, focal adhesion kinase, and GTPase KRas.

increase was not statistically significant, it suggests an adaptive response to oxidative stress (Fig. 7B). Similarly, p21 showed upregulation at 61 µg/mL, with an expression level of 1.70 ± 0.05, reflecting a response related to cell cycle regulation (Fig. 7C). Furthermore, p53 expression was significantly elevated at 61 µg/mL and 81 µg/mL concentrations, reaching 2.71 ± 0.29 and 2.15 ± 0.26 ($P < 0.05$), which reinforces its role in the cellular stress response (Fig. 7D). These results suggest that 4-FOC-conjugated NCC/CTAB/CS NPs can modulate the expression of key genes involved in apoptosis and cell cycle regulation in PANC-1 cells, with effects that vary depending on the concentration used.

Antioxidant capacity assay

The antioxidant capacity of the 4-FOC-conjugated NCC/CTAB/CS NPs was evaluated by their ability to scavenge ABTS and DPPH free radicals. The results showed a significant concentration-dependent increase in radical scavenging activity in both assays (Fig. 8; $P < 0.001$). The ABTS radical scavenging activity steadily increased with the concentration of the NPs, reaching 38.82% at the highest concentration of 2000 µg/mL. Similarly, the DPPH radical scavenging activity also increased with NP concentration, achieving 68.25% at the highest concentration. These findings indicate that the 4-FOC-conjugated NCC/CTAB/CS NPs possess noticeable antioxidant properties, as demonstrated by their effectiveness in scavenging both ABTS and DPPH free radicals in a concentration-dependent manner.

Docking analysis

Molecular docking analysis demonstrates that the 4-FOC-conjugated NCC/CTAB/CS NP molecule exhibits the highest binding affinity and lowest S-score for the GTPase KRas protein (− 7.91). Furthermore, 4-FOC displays low binding scores for the Focal Adhesion Kinase and Snail1 proteins, as reported in Table 2. The interactions of these binding occurrences are depicted in Fig. 9. These results indicate the potential for the 4-FOC to influence the PANC-1 cell line.

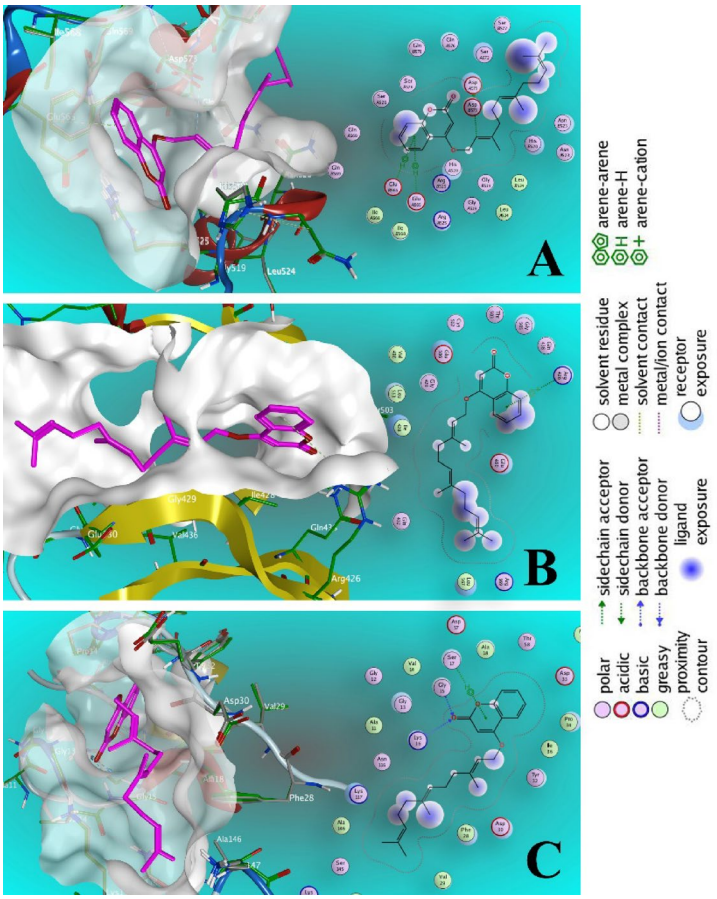

Fig. 9. The figure illustrates the interactions between the Snail1, Focal Adhesion Kinase, GTPase KRas proteins, and the compound 4-farnesyloxycoumarin (4-FOC) in the PANC-1 cell line. Part A depicts the interaction of Snail1 with this compound, while Part B elucidates the interaction of Focal Adhesion Kinase. Lastly, part C demonstrates the interaction of GTPase KRas with this compound.

Discussion

Targeted therapy represents a transformative advancement in oncology. It provides a tailored approach that selectively targets neoplastic cells while sparing adjacent healthy tissue unharmed[26]. Unlike conventional chemotherapy, which indiscriminately impacts both malignant and normal cells, targeted therapy leverages the distinctive molecular and genetic aberrations inherent to cancer cells. This specificity enhances therapeutic efficacy and mitigates adverse effects, improving clinical outcomes[27]. The development of DDSs plays a crucial role in the success of targeted therapies. Optimal drug delivery mechanisms facilitate the precise localization of therapeutics at the tumor microenvironment, thereby increasing local drug concentration and minimizing systemic exposure[28]. Such targeted administration amplifies the therapeutic index and lowers the incidence of off-target effects, thereby enhancing the overall safety profile of treatment regimens[29]. Ongoing advancements in drug delivery technologies, such as NPs, liposomes, and antibody-drug conjugates, are essential for refining the delivery of targeted therapies[28]. These innovations are vital for increasing the effectiveness of cancer treatment strategies, highlighting the importance of continued research and development in this area.

Our study explored the effects of 4-FOC-conjugated NCC/CTAB/CS NPs on PANC-1 cancer cells. 4-FOC is a coumarin derivative with potential therapeutic applications in cancer treatment. Herbal compounds, especially secondary metabolites, are attractive in oncology due to their anti-cancer properties and lower side effects[30,31]. Many clinically approved anti-cancer therapeutics are derived from natural products, highlighting their potential as a source for novel oncological agents. For example, alkaloids such as vincristine and vinblastine[32] are sourced from the periwinkle plant, while camptothecin derivatives like irinotecan come from the Camptotheca tree, etoposide is derived from the mayapple[33], and paclitaxel is obtained from the Pacific yew tree[34]. These compounds are vital for cancer treatment and continue to inspire research aimed at discovering new therapeutics that offer improved efficacy and safety. Building on this foundation, our objective in this study was to enhance the therapeutic properties of 4-FOC by using NCC/CTAB/CS NPs. According to the DLS assay results, the synthesized NPs have favorable characteristics for drug delivery applications, including moderate particle size, narrow size distribution, and good stability. These properties suggest that the NPs can effectively facilitate targeted delivery, as reflected by the polydispersity index and zeta potential values. Additionally, smaller particles within the sample may enhance the NPs' efficacy in reaching and penetrating

tumor sites. FESEM analysis offered essential insights into the physical characteristics of the NPs, confirming successful conjugation and emphasizing their nanoscale nature. The observed heterogeneous size distribution indicates variability in aggregation processes, which could impact drug release dynamics and cellular uptake efficiency. FTIR spectroscopy confirmed the successful synthesis of 4-FOC-conjugated NCC/CTAB/CS NPs by identifying characteristic functional groups and structural features. The presence of hydroxyl, carbonyl, and aromatic groups supports the integration of necessary functional components for effective drug delivery. Encapsulation efficiency was significantly high at 88.49%, demonstrating the successful incorporation of 4-FOC into the NPs. This high efficiency ensures that a substantial amount of the therapeutic agent reaches the target cells, thereby improving treatment efficacy. The cytotoxicity assay showed a dose-dependent decrease in the viability of PANC-1 cells, with significant effects noted at higher concentrations. The IC50 value of 61.23 µg/mL indicates that the 4-FOC-conjugated NCC/CTAB/CS NPs have suitable cytotoxicity for targeting cancer cells while still maintaining some level of selectivity, as demonstrated by the greater tolerance observed in HDF cells. The apoptotic assays, which included Annexin V-FITC/PI and AO/PI staining, revealed that the NPs effectively induce apoptosis in PANC-1 cells in a concentration-dependent manner. These results are further validated by DAPI staining, which showed typical signs of apoptosis, such as nuclear condensation and fragmentation. Gene expression analysis revealed that essential genes involved in apoptosis and cell cycle regulation, such as caspase 3, p21, and p53, were upregulated. These findings indicate that the 4-FOC-conjugated NCC/CTAB/CS NPs influence cellular pathways to promote apoptosis and respond to oxidative stress, enhancing their therapeutic potential. Lastly, the antioxidant capacity assay demonstrated significant radical scavenging activity, indicating that the 4-FOC-conjugated NCC/CTAB/CS NPs possess notable antioxidant properties. This ability to scavenge free radicals further supports their potential role in cancer therapy by reducing oxidative stress within tumor environments. The molecular docking results indicate that 4-FOC binds to Focal Adhesion Kinase 1, GTPase KRas, and Snail1 in PANC-1 cells, with a particularly high affinity for GTPase KRas based on the S-score and amino acid interactions. Activating mutations in the KRas gene are crucial for pancreatic cancer development and treatment resistance[35,36]. These alterations activate the Ras signaling pathway, promoting tumor cell proliferation and survival[37]. Inhibiting KRas shows promise as a therapeutic strategy, with novel pan-KRas inhibitors effective against various KRas mutations[38]. Krishnamurthy et al. found that curcumin analogs and curcumin-biphenyl carbonitrile conjugates targeted the KRas oncogene and showed anti-cancer activity against the PANC-1 cell line, achieving a binding score of − 6.810[39]. In contrast, this study shows a binding score of − 7.91 for 4-FOC, suggesting a superior inhibitory effect. The 4-FOC-conjugated NCC/CTAB/CS NPs represent a promising platform for targeted drug delivery in pancreatic cancer treatment. This approach offers enhanced efficacy through selective targeting, induction of apoptosis, and antioxidant activity.

Previous studies have shown that FOC derivates exhibit various biological activities, making them candidates for further oncology investigation[40]. For instance, evidence suggests that FOC derivatives, including 8-FOC, 7-FOC, and 5-FOC, may be promising anti-cancer agents for prostate cancer by targeting the overexpressed enzyme 15-lipoxygenase-1 (15-LOX-1). These compounds have shown significant cytotoxic effects in PC-3 prostate cancer cells, leading to apoptosis and DNA damage while sparing normal human foreskin fibroblast cells (HFF3). Additionally, the ability of these derivatives to induce G1 cell cycle arrest further highlights their therapeutic potential[17,20,41]. Research on various coumarin analogs has also shown their ability to inhibit cell proliferation in human breast cancer cell lines while sparing healthy fibroblasts, suggesting a targeted action against cancer cells[42].

FOC derivates can trigger apoptosis through various pathways. They can activate caspases and influence cell cycle regulators such as p53 and cyclin D1, leading to cancer cell apoptosis[43]. Furthermore, FOC derivates may impact key signaling pathways in cancer progression, including the PI3K/Akt/mTOR and ERK1/2 pathways[43]. These pathways are critical for cell survival and proliferation, and their inhibition can lead to reduced tumor growth. Some studies suggest that coumarins can inhibit angiogenesis, which is essential for tumor growth and metastasis[44]. As a result, there is growing interest in using coumarin derivates as adjuncts to conventional cancer therapies. Their ability to enhance the efficacy of chemotherapeutic agents while potentially reducing side effects makes them valuable candidates for combination treatments[45]. Furthermore, compounds like 4-FOC may play a role in cancer prevention by inhibiting the initiation and progression of cancerous changes at the cellular level[46]. Research indicates that the cytotoxic effects of FOC compounds are dose-dependent, with higher concentrations leading to more significant reductions in cancer cell viability[43]. Moreover, the farnesyl and other lipophilic groups enhance the biological activity of coumarins by increasing their solubility and bioavailability[42,46].

In summary, FOC derivates represent a promising cancer treatment due to its multifaceted mechanisms of action, including the inhibition of tumor growth, induction of apoptosis, and modulation of critical signaling pathways. In this context, our study highlights the potential of 4-FOC-conjugated NCC/CTAB/CS NPs as a targeted drug delivery system for cancer therapy. Although this study offers insights into the effects of 4-FOC-conjugated NCC/CTAB/CS NPs on PANC-1 cells, several limitations should be considered. Firstly, the in vitro nature of the experiments may only partially replicate the complex tumor microenvironment typically found in vivo, which could impact the translation of these findings to clinical settings. Furthermore, additional research is necessary to investigate these NPs' long-term effects, potential toxicity in normal tissues, pharmacokinetics, and biodistribution in vivo. Future studies could benefit from testing a broader range of cancer cell lines to evaluate the specificity and efficacy of the treatment across different cancer types.

Conclusion

In conclusion, the study demonstrates that 4-FOC-conjugated NCC/CTAB/CS NPs exhibit significant cytotoxic effects on PANC-1 cells. This is evidenced by a reduction in cell viability and an increase in apoptotic activity in a concentration-dependent manner. The NPs effectively encapsulate 4-FOC, achieving an impressive efficiency of 88.49%. Additionally, they possess notable antioxidant properties, as shown by their ability to scavenge ABTS

and DPPH free radicals. Gene expression analysis further supports the mechanism of action, revealing the upregulation of critical apoptotic and cell cycle regulatory genes, such as caspase 3, p53, and p21, in response to treatment. These findings highlight the potential of 4-FOC-conjugated NCC/CTAB/CS NPs as a promising therapeutic strategy for pancreatic cancer, warranting further investigation into their in vivo efficacy and safety profiles.

Data availability

The datasets used and/or analyzed during the current study are available from the corresponding author upon reasonable request.

Received: 13 January 2025; Accepted: 13 May 2025
Published online: 19 May 2025

References

1. Lee, Y. T., Tan, Y. J. & Oon, C. E. Molecular targeted therapy: Treating cancer with specificity. *Eur. J. Pharmacol.* **834**, 188–196 (2018).
2. Schirrmacher, V. From chemotherapy to biological therapy: A review of novel concepts to reduce the side effects of systemic cancer treatment. *Int. J. Oncol.* **54**(2), 407–419 (2019).
3. Lin, Q. et al. Advancing ovarian Cancer therapeutics: The role of targeted drug delivery systems. *Int. J. Nanomed.* 9351–9370 (2024).
4. Khan, M. I. et al. Recent progress in nanostructured smart drug delivery systems for cancer therapy: A review. *ACS Appl. Bio Mater.* **5**(3), 971–1012 (2022).
5. Liu, G. et al. A review on drug delivery system for tumor therapy. *Front. Pharmacol.* **12**, 735446 (2021).
6. Qian, J. et al. Combination of micelles and liposomes as a promising drug delivery system: A review. *Drug Deliv. Transl. Res.* **13**(11), 2767–2789 (2023).
7. Abitbol, T., Marway, H. & Cranston, E. D. Surface modification of cellulose nanocrystals with cetyltrimethylammonium bromide. *Nord. Pulp Pap. Res. J.* **29**(1), 46–57 (2014).
8. Zainuddin, N., Ahmad, I., Zulfakar, M. H., Kargarzadeh, H. & Ramli, S. Cetyltrimethylammonium bromide-nanocrystalline cellulose (CTAB-NCC) based microemulsions for enhancement of topical delivery of Curcumin. *Carbohydr. Polym.* **254**, 117401 (2021).
9. Richardo, L. P. & Nugraha, V. A. *Modifications of Nanocrystalline Cellulose with Chitosan for Controlled Release of Drug* (Faculty of Engineering, 2016).
10. Babaei-Ghazvini, A., Patel, R., Vafakish, B., Yazdi, A. F. A. & Acharya, B. Nanocellulose in targeted drug delivery: A review of modifications and synergistic applications. *Int. J. Biol. Macromol.* 135200 (2024).
11. Karimian, A. et al. Nanocrystalline cellulose: Preparation, physicochemical properties, and applications in drug delivery systems. *Int. J. Biol. Macromol.* **133**, 850–859 (2019).
12. Soltani, M. et al. Folic acid-modified nanocrystalline cellulose for enhanced delivery and anti-cancer effects of Crocin. *Sci. Rep.* **14**(1), 13985 (2024).
13. Liang, X., Mu, M., Fan, R., Zou, B. & Guo, G. Functionalized Chitosan as a promising platform for cancer immunotherapy: A review. *Carbohydr. Polym.* **290**, 119452 (2022).
14. Smith, J., Wood, E. & Dornish, M. Effect of Chitosan on epithelial cell tight junctions. *Pharm. Res.* **21**, 43–49 (2004).
15. Küpeli Akkol, E., Genç, Y., Karpuz, B., Sobarzo-Sánchez, E. & Capasso, R. Coumarins and coumarin-related compounds in pharmacotherapy of cancer. *Cancers* **12**(7), 1959 (2020).
16. Sargolzaei, J., Sadeghian, H., Golahmadi, S. & Soukhtanloo, M. Cytotoxic effects of hydroxy coumarin derivatives on mouse neuroblastoma N2a cell line: Effects of hydroxy coumarin derivations in N2A cell line. *Iran. J. Pharm. Sci.* **16**(3), 95–106 (2020).
17. Hosseinymehr, M., Matin, M. M., Sadeghian, H., Bahrami, A. R. & Kaseb-Mojaver, N. 8-Farnesyloxycoumarin induces apoptosis in PC-3 prostate cancer cells by Inhibition of 15-lipoxygenase-1 enzymatic activity. *Anti-Cancer Drugs* **27**(9), 854–862 (2016).
18. Matos, M. J. et al. Coumarins—An important class of phytochemicals. *Phytochemicals-isolation Characterisation Role Hum. Health* **25**, 533–538 (2015).
19. Lyndem, S. et al. A comprehensive in vitro exploration into the interaction mechanism of coumarin derivatives with bovine hemoglobin: Spectroscopic and computational methods. *J. Photochem. Photobiol. A* **436**, 114425 (2023).
20. Saboormaleki, S., Sadeghian, H., Bahrami, A. R., Orafaie, A. & Matin, M. M. 7-Farnesyloxycoumarin exerts anti-cancer effects on a prostate cancer cell line by 15-LOX-1 Inhibition. *Arch. Iran. Med.* **21**(6), 251–259 (2018).
21. Kirsch, G., Abdelwahab, A. B. & Chaimbault, P. Natural and synthetic coumarins with effects on inflammation. *Molecules* **21**(10), 1322 (2016).
22. Mekjaruskul, C., Sungthong, B., Puthongking, P. & Boonyarat, C. Pharmacokinetics and oral bioavailability of coumarins and carbazole alkaloids from Clausena harmandiana root bark in rats. *Revista Brasileira De Farmacognosia* **33**(6), 1170–1176 (2023).
23. Abraham, K., Pfister, M., Wöhrlin, F. & Lampen, A. Relative bioavailability of coumarin from cinnamon and cinnamon-containing foods compared to isolated coumarin: A four-way crossover study in human volunteers. *Mol. Nutr. Food Res.* **55**(4), 644–653 (2011).
24. Celebi, H. & Kurt, A. Effects of processing on the properties of Chitosan/cellulose nanocrystal films. *Carbohydr. Polym.* **133**, 284–293 (2015).
25. Namvar, F. et al. Green synthesis, characterization, and anti-cancer activity of hyaluronan/zinc oxide nanocomposite. *OncoTargets Therapy* 4549–4559 (2016).
26. Zhong, L. et al. Small molecules in targeted cancer therapy: Advances, challenges, and future perspectives. *Signal. Transduct. Target. Therapy* **6**(1), 1–48 (2021).
27. Tsimberidou, A-M. Targeted therapy in cancer. *Cancer Chemother. Pharmacol.* **76**, 1113–1132 (2015).
28. Adepu, S. & Ramakrishna, S. Controlled drug delivery systems: Current status and future directions. *Molecules* **26**(19), 5905 (2021).
29. Ezike, T. C. et al. Advances in drug delivery systems, challenges and future directions. *Heliyon* **9**(6) (2023).
30. Sharma, A. et al. Molecular aspects and therapeutic implications of herbal compounds targeting different types of cancer. *Molecules* **28**(2), 750 (2023).
31. Ali, M. et al. Recent advance of herbal medicines in cancer-a molecular approach. *Heliyon* **9**(2) (2023).
32. Paul, A., Acharya, K. & Chakraborty, N. Biosynthesis, extraction, detection and pharmacological attributes of vinblastine and vincristine, two important chemotherapeutic alkaloids of *Catharanthus roseus* (L.) G. Don: A review. *South. Afr. J. Bot.* **161**, 365–376 (2023).
33. Kamle, M. et al. Camptothecin and its derivatives: Advancements, mechanisms and clinical potential in cancer therapy. *Med. Oncol.* **41**(11), 263 (2024).
34. Tong, Z. *Research Study Finds Alternative to Scarce Yew-Tree Source for Top Anti-cancer Drug*. (South China Morning Post, 2024).

35. Luo, J. (ed) *Editor KRAS Mutation in Pancreatic Cancer. Seminars in Oncology* (Elsevier, 2021).
36. Zhang, Z., Zhang, H., Liao, X. & Tsai, H. KRAS mutation: The booster of pancreatic ductal adenocarcinoma transformation and progression. *Front. Cell. Dev. Biol.* **11**, 1147676 (2023).
37. Kim, H. J., Lee, H. N., Jeong, M. S. & Jang, S. B. Oncogenic KRAS: Signaling and drug resistance. *Cancers* **13**(22), 5599 (2021).
38. Kim, D. et al. Pan-KRAS inhibitor disables oncogenic signalling and tumour growth. *Nature* **619**(7968), 160–166 (2023).
39. Krishnamurthy, G. et al. Study of in-silico ADMET, molecular docking, and stability potential of synthesized novel tetrazole bearing curcumin derivatives and evaluation of their anti-cancer potential on PANC-1 cell lines. *Rasayan J. Chem.* **16**(1), 335–354 (2023).
40. Bhattarai, N., Kumbhar, A. A., Pokharel, Y. R. & Yadav, P. N. Anti-cancer potential of coumarin and its derivatives. *Mini Rev. Med. Chem.* **21**(19), 2996–3029 (2021).
41. Orafaie, A., Sadeghian, H., Bahrami, A. R., Saboormaleki, S. & Matin, M. M. 5-Farnesyloxycoumarin: A potent 15-LOX-1 inhibitor, prevents prostate cancer cell growth. *Med. Chem. Res.* **26**, 227–234 (2017).
42. Gkionis, L. et al. Investigation of the cytotoxicity of bioinspired coumarin analogues towards human breast cancer cells. *Mol. Diversity* **25**, 307–321 (2021).
43. Shakiba, M. & Rassouli, F. B. Joining up the scattered anti-cancer knowledge on auraptene and umbelliprenin: A meta-analysis. *Sci. Rep.* **14**(1), 11770 (2024).
44. Majnooni, M. B. et al. Antiangiogenic effects of coumarins against cancer: From chemistry to medicine. *Molecules* **24**(23), 4278 (2019).
45. Kostova, I. Synthetic and natural coumarins as cytotoxic agents. *Curr. Med. Chem. Anti-Cancer Agents* **5**(1), 29–46 (2005).
46. Annunziata, F., Pinna, C., Dallavalle, S., Tamborini, L. & Pinto, A. An overview of coumarin as a versatile and readily accessible scaffold with broad-ranging biological activities. *Int. J. Mol. Sci.* **21**(13), 4618 (2020).

Acknowledgements
We sincerely thank the Vice Chancellor of Research of Islamic Azad University of Shahrood for supporting and facilitating this research.

Author contributions
Fariba Karoonkiani: Investigation, Methodology and Writing-Original draft. Masoud Homayouni Tabrizi, Mohammad Taghi Goodarzi, Alireza Jalali: Supervision, Data curation, Conceptualization Software, Validation, and Writing Reviewing.

Funding
This research received no specific grant from any funding agency in the public, commercial, or not-for-profit sectors.

Declarations

Competing interests
The authors declare no competing interests.

Additional information
Correspondence and requests for materials should be addressed to M.H.T.

Reprints and permissions information is available at www.nature.com/reprints.

Publisher's note Springer Nature remains neutral with regard to jurisdictional claims in published maps and institutional affiliations.